Electronic Supplementary Information

Carbon block anodes with columnar nanopores constructed from amine-functionalized carbon nanosheets for sodium-ion batteries

Yue Zhang,[a] Zihe Zhang,[b] Yakun Tang,[a] Dianzeng Jia,[*a] Yudai Huang,[a] Yong Guo[a] and Zhen Zhou[*bc]

[a] *Key Laboratory of Energy Materials Chemistry, Ministry of Education; Key Laboratory of Advanced Functional Materials, Autonomous Region; Institute of Applied Chemistry, School of Chemistry, Xinjiang University, Urumqi, 830046, Xinjiang, China.*

Email: jdz@xju.edu.cn

[b] *School of Materials Science and Engineering, Institute of New Energy Material Chemistry, Nankai University, Tianjin 300350, China.*

E-mail: zhouzhen@nankai.edu.cn

[c] *Engineering Research Center of Advanced Functional Material Manufacturing of Ministry of Education, School of Chemical Engineering, Zhengzhou University, Zhengzhou 450001, China*

Computational Details: DFT computations were performed within Vienna ab initio simulation package (VASP).[1] We adopted projector augmented wave (PAW) potentials and Perdew-Burke-Ernzerhof (PBE) exchange and correlation functional.[2,3] The energy cutoff was set as 450 eV for the plane-wave basis set. DFT-D3 method with Becke-Johnson damping was also employed to evaluate the van der Waals interaction more precisely.[4] The structures of pristine and amine-modified graphite bulk and surface were used to investigate the effect of amine groups. The bulk structure was modeled by a 4×4×1 graphite supercell, and the surface structure was simulated by a 4-layer 4×4 supercell with ~15 Å vacuum in the z direction. The 4×4×4 and 4×4×1 K-point meshes were used to sample the Brillouin zone of bulk and surface structures, respectively. The differential charge density $\Delta\rho$ was computed as:

$$\Delta\rho = \rho_{ad} - \rho_{graphite} - \rho_{Na}$$

where ρ_{ad} represents the electron density of the structure of Na adsorption on graphite host, $\rho_{graphite}$ and ρ_{Na} are the electron density of the graphite host and Na atom, respectively. The Fig. 5 of differential charge density were generated by VESTA.[5]

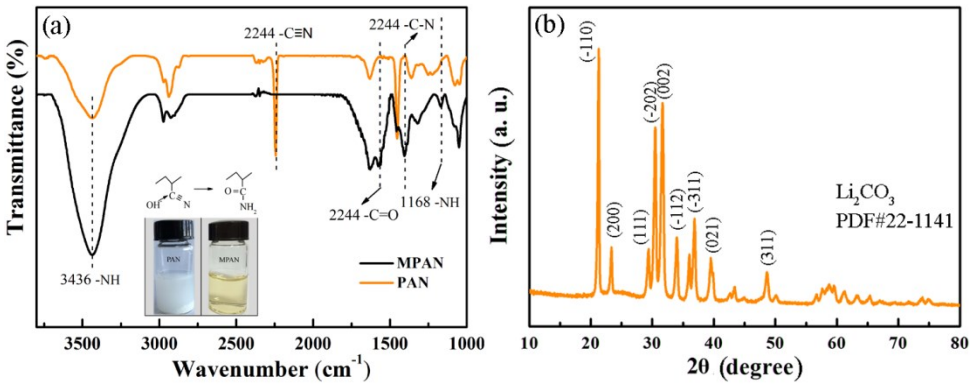

Fig. S1 (a) FT-IR spectra of PAN and MPAN with inset of their corresponding optical photographs. (b) XRD patterns of the AFPC precursor after carbonization without acid treatment.

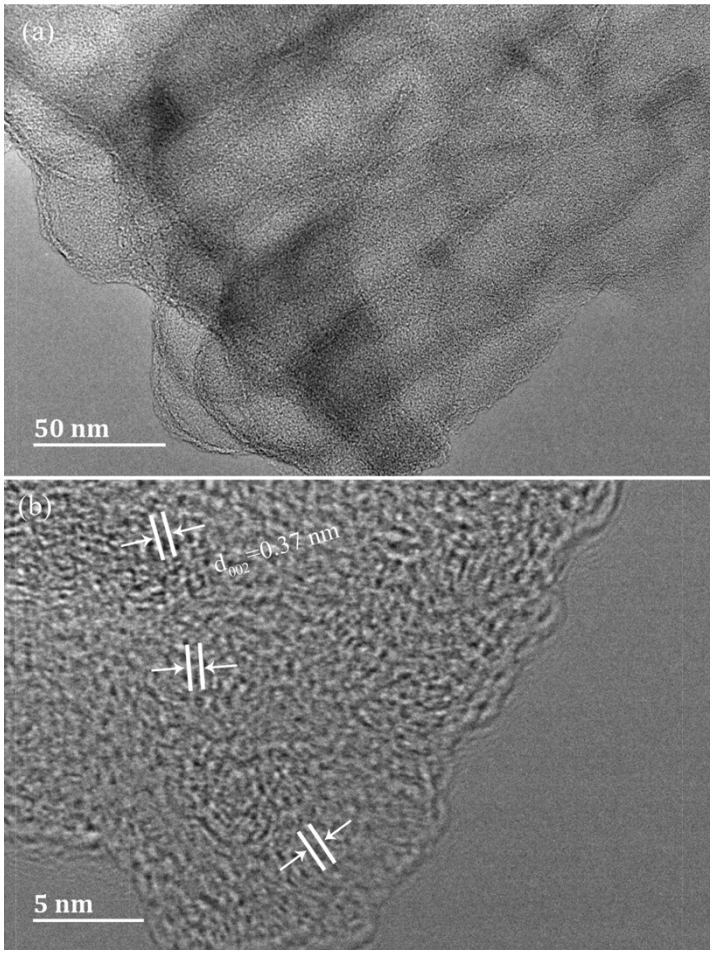

Fig. S2 (a, b) HRTEM images of AFPC with different magnification.

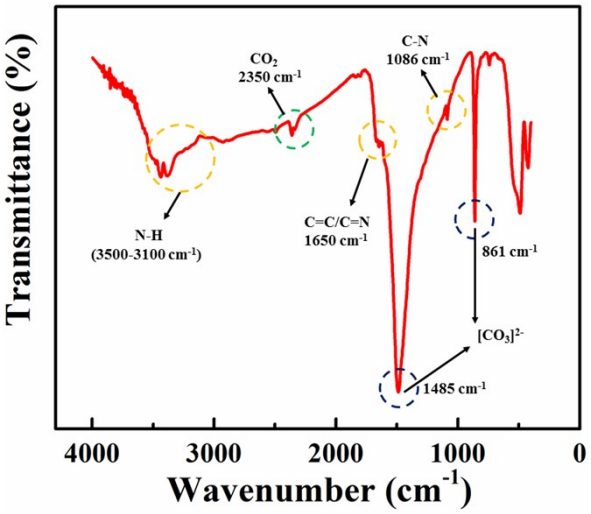

Fig. S3 FTIR spectrum of AFPC before removing the template.

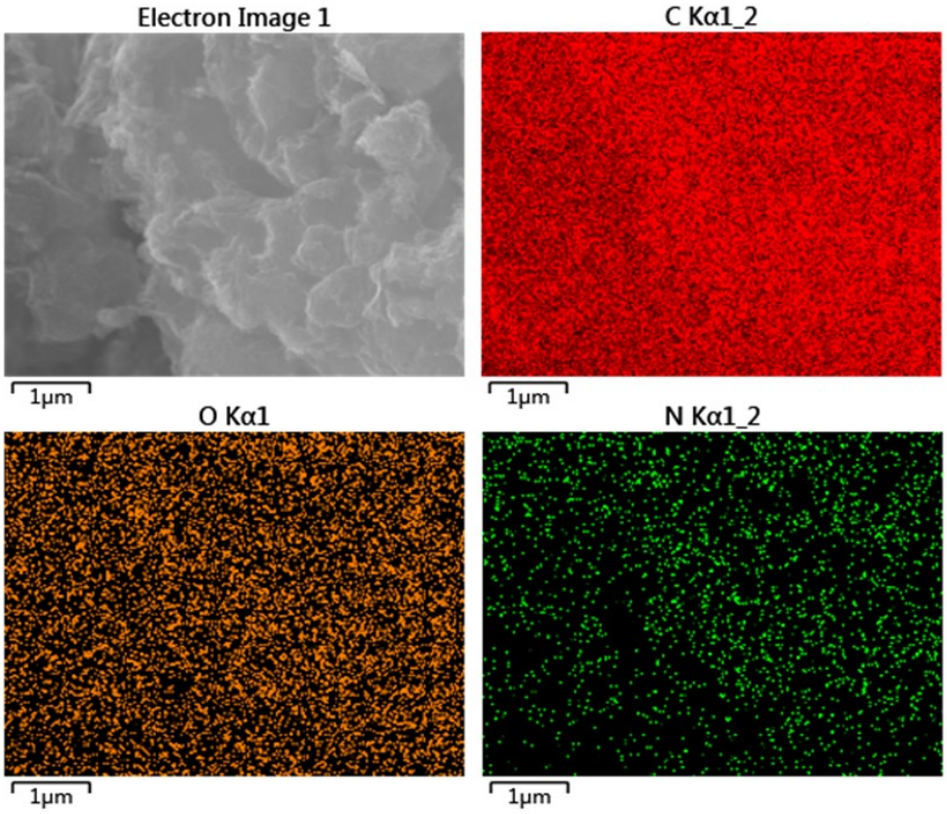

Fig. S4 SEM image and corresponding C, O, and N element mapping of AFPC.

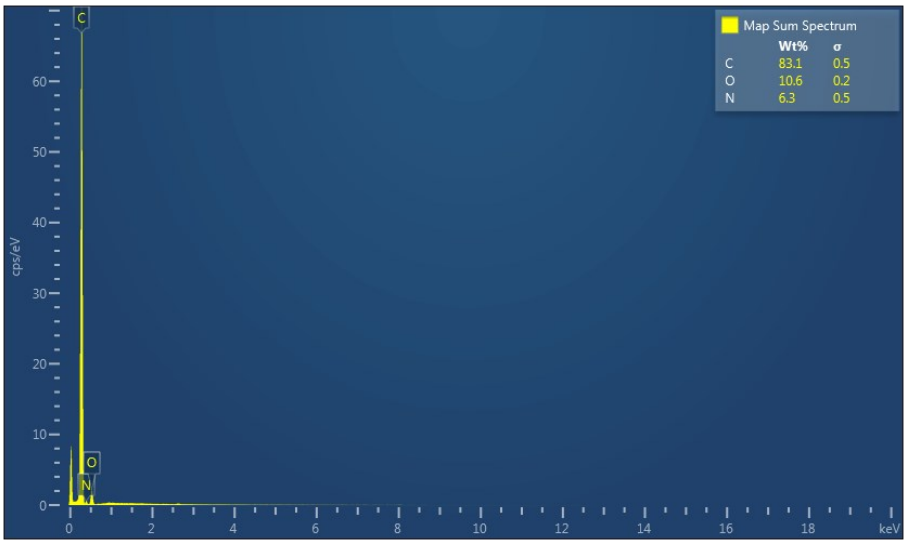

Fig. S5 EDX quantitative analysis of AFPC.

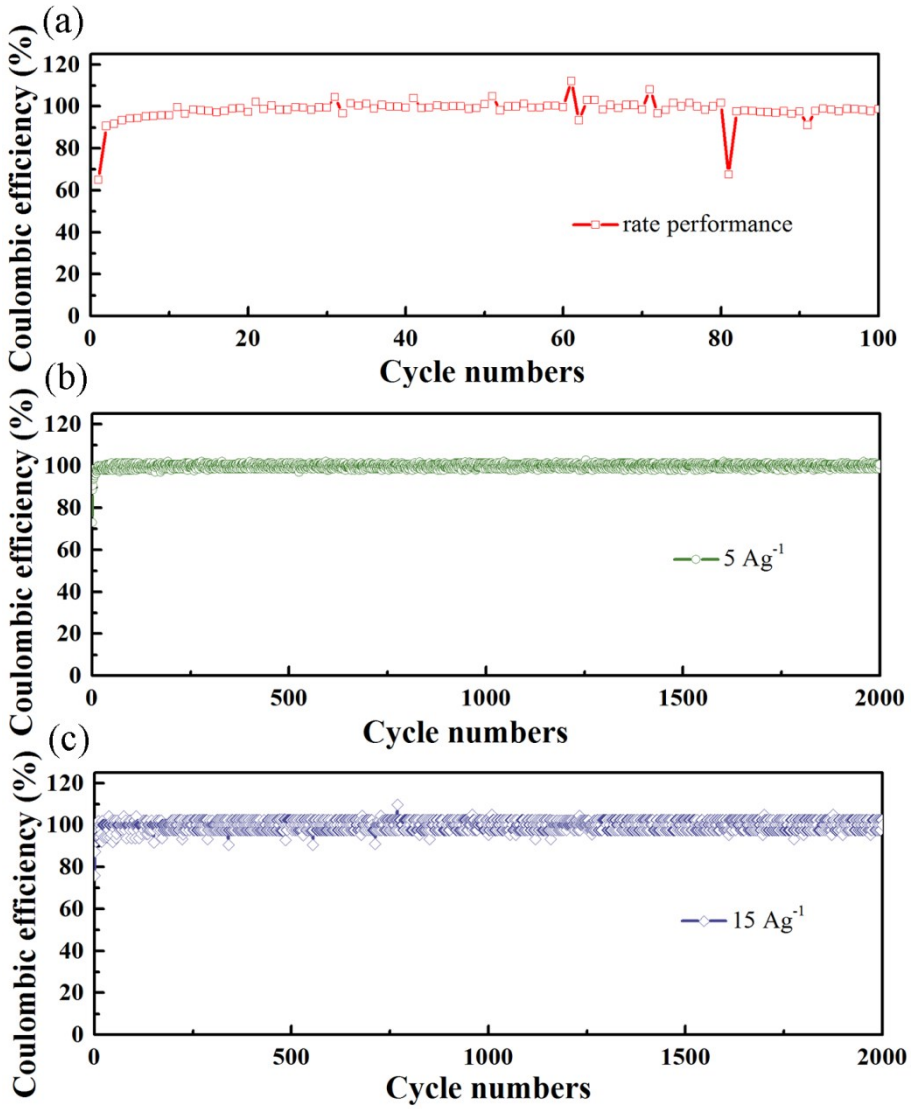

Fig. S6 Coulombic efficiencies corresponding to Fig. 6e (a) and Fig. 6f (b, c).

Table S1 A survey of electrochemical performances of similar materials reported in the open literatures.

Typical materials	Current density	Cycle numbers	Remaining capacity (mAh g^{-1})	High rate performance (mAh g^{-1})	Ref.
Sulphur-doped carbon nanosheets	5 A g^{-1}	2000	211	170 (5 A g^{-1}) 127 (10 A g^{-1})	6
Heteroatom doping carbon nanofibers	10 A g^{-1}	6000	164.3	152 (5 A g^{-1}) 149 (10 A g^{-1})	7
N-rich porous carbon nanosheets	5 A g^{-1}	1000	170	215 (5 A g^{-1}) 194 (10 A g^{-1})	8
N, P-dual doping carbon sheets	1 A g^{-1}	2000	103	143 (1 A g^{-1}) 122 (2 A g^{-1})	9
Nitrogen-doped wrinkled carbon foils	1 A g^{-1}	1000	188	175 (5 A g^{-1}) 150 (10 A g^{-1})	10
N-doped amorphous carbon nanofibers	1 A g^{-1}	8000	105	180 (0.5 A g^{-1}) 121 (1 A g^{-1})	11
N/S co-doped ordered mesoporous carbon	5 A g^{-1}	3000	220	292 (2 A g^{-1}) 233 (5 A g^{-1})	12
Nitrogen-rich hierarchically porous carbon	0.5 A g^{-1} 5 A g^{-1}	3000 10000	260 101.4	174 (1 A g^{-1}) 150 (2 A g^{-1})	13
S-doped Graphene	2 A g^{-1}	1000	250	251 (1.6 A g^{-1}) 217 (3.2 A g^{-1})	14
Heteroatom-doped hollow aurilave-like structured carbon	0.2 A g^{-1} 1 A g^{-1}	100 1000	199 185	77 (5 A g^{-1}) 45 (10 A g^{-1})	15
In situ high-level amine-functionalized carbon material	5 A g^{-1} 15 A g^{-1}	2000 2000	201 175	211 (5 A g^{-1}) 192 (10 A g^{-1})	This work

References

[1] K. Chayambuka, G. Mulder, D. L. Danilov and P. H. L. Notten, *Adv. Energy Mater.*, 2018, **8**, 1800079

[2] G. Kresse and J. Furthmüller, *Phys. Rev. B*, 1996, **54**, 11169.

[3] G. Kresse and D. Joubert, *Phys. Rev. B*, 1999, **59**, 1758-1775; J. P. Perdew, K. Burke and M. Ernzerhof, *Phys. Rev. Lett.*, 1996, **77**, 3865-3868.

[4] S. Grimme, J. Antony, S. Ehrlich and H. Krieg, *J. Chem. Phys.*, 2010, **132**, 154104; S. Grimme, S. Ehrlich and L. Goerigk, *J. Comput. Chem.*, 2011, **32**, 1456.

[5] K. Momma and F. Izumi, *Appl. Crystallogr.*, 2011, **44**, 1272.

[6] G. Y. Zhao, D. F. Yu, H. Zhang, F. F. Sun, J. W. Li, L. Zhu, L. Sun, M. Yu, F. Besenbacher and Y. Sun, *Nano Energy*, 2020, **67**, 104219.

[7] Y. Bao, Y. P. Huang, X. Song, J. Long, S. Q. Wang, L. X. Ding and H. H. Wang, *Electrochim. Acta*, 2018, **276**, 304-310.

[8] S. T. Liu, J. S. Zhou and H. H. Song, *Adv. Energy Mater.*, 2018, **8**, 1800569.

[9] D. C. Qin, Z. Y. Liu, Y. Z. Zhao, G. Y. Xu, F. Zhang and X. G. Zhang, *Carbon* 2018, **130**, 664-671.

[10] L. J. Kong, J. Zhu, W. Shuang and X. H. Bu, *Adv. Energy Mater.*, 2018, **8**, 1801515.

[11] R. Hao, Y. Yang, H. Wang, B. B. Jia, G. S. Ma, D. D. Yu, L. Guo and S. H. Yang, *Nano Energy*, 2018, **45**, 220.

[12] J. Q. Ye, H. Q. Zhao, W. Song, N. Wang, M. M. Kang and Z. Li, *J. Power Sources*, 2019, **412**, 606.

[13] X. D. Hu, X. H. Sun, S. J. Yoo, B. Evankod, F. R. Fan, S. Cai, C. M. Zheng, W. B. Hu and G. D. Stucky, *Nano Energy*, 2019, **56**, 828.

[14] B. Quan, A. Jin, S. H. Yu, S. M. Kang, J. Jeong, H. D. Abruña, L. Y. Jin, Y. Z. Piao and Y. E. Sung, *Adv. Sci.*, 2018, **5**, 1700880.

[15] Q. J. Sun, Z. Cao, S. H. Wang, L. S. Sun, L. Zhou, H. J. Xue, Y. Q. Wu, L. Cavallo, L. M. Wang and J. Ming, *J. Power Sources*, 2020, **461**, 228128.